Politechnika Warszawska

Wydział Mechaniczny Energetyki i Lotnictwa

Zakład Silników Lotniczych

Metody Komputerowe w Spalaniu

Flow and Combustion Simulation in Hydrogen-Adapted Combustion Chamber for GTM-140 Miniature Turbine Engine

Bartłomiej Maślach

Instructor: dr inż. Mateusz Żbikowski

Date of Submission: **15.05.2025**

1 Introduction and Motivation

The transition to sustainable energy sources has become important point of global policy, with hydrogen emerging as an alternative for decarbonization. The aviation industry is a significant contributor to global emissions. The remedy for that could be Hydrogen fuel, whether used in fuel cells or as a direct combustion fuel, offering a transformation opportunity for achieving zero-emission flights. This research explores the possibility od adapting currently used hydrogen turbine engines to work with gaseous hydrogen as a fuel. The report is a part of KNN Melprop's students organization Hydrogen Turbine Engine Project with main goal to asses the chances for developing relatively affordable solution for Jet A1 to Hydrogen conversion.

2 Geometry Adaptation

GTM-140 is a miniature turbine engine produced by JETPOL. In its default configuration GTM-140 is equipped with single stage centrifugal compressor (compression ratio 2.8), and single stage axial turbine. At 100% speed (120000 rpm), GTM-140 generates 140N of static thrust. The combustion chamber is of an annular type with 12 vaporizers and injectors, enabling evaporation and proper mixing of JetA1 fuel. The direction of the flow inside the vaporizer is opposed to so that the overall size of the combustion chamber can be reduced due to the extended flow path.

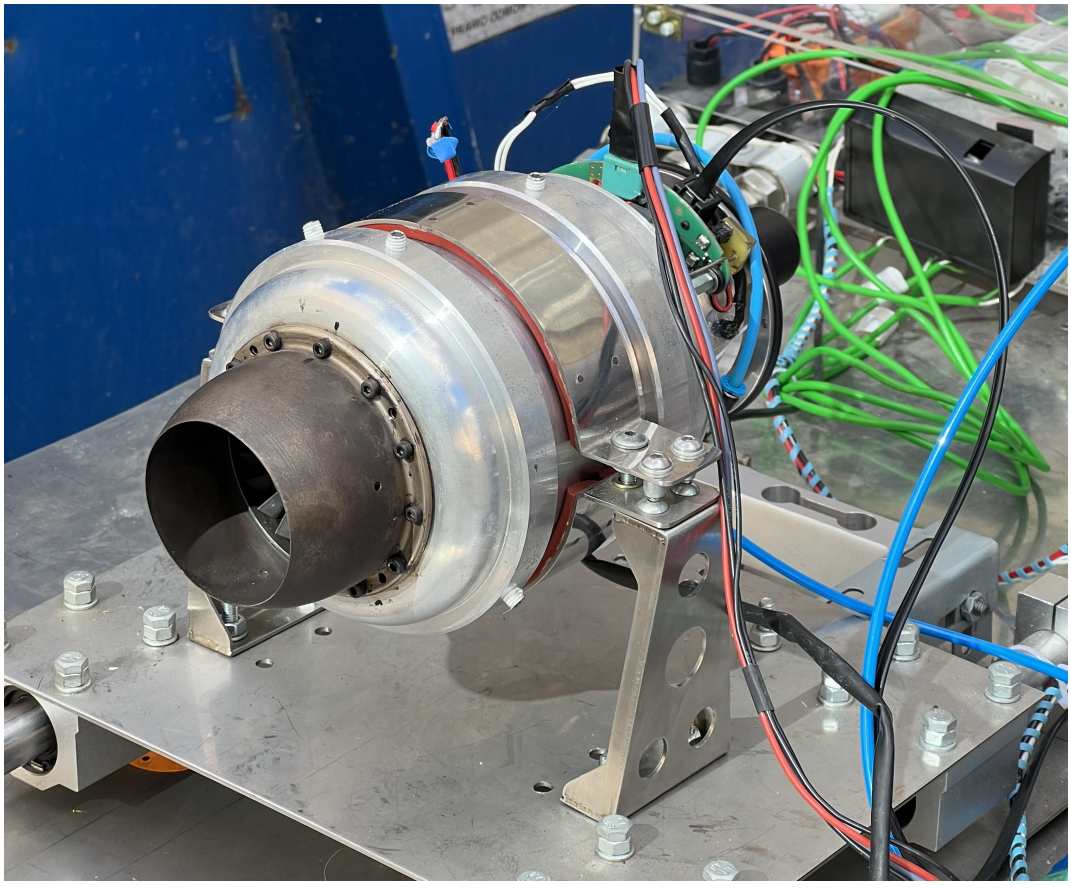

Fig 2.1 GTM 140 miniature turbine engine

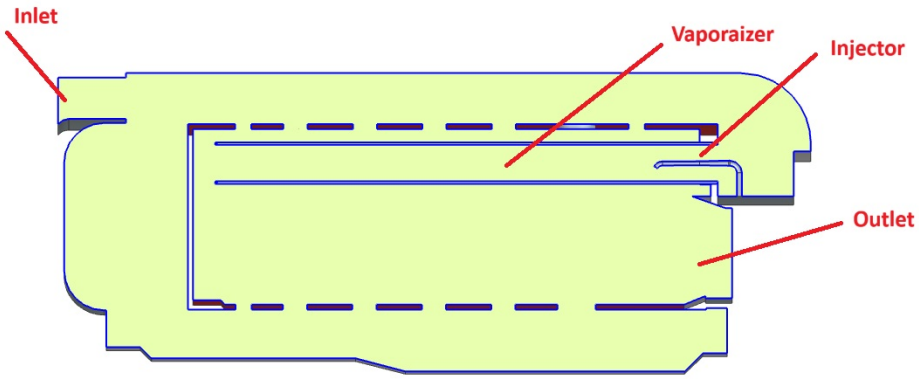

Fig 2.2 Cross-section of a axis-symmetric annular combustion chamber - body of fluid

One of the project assumptions is to minimize the geometry changes to maintain existing infrastructure and to optimize hydrogen conversion costs, therefore new design with only essential changes was proposed.

Following changes of geometry were introduced:

- removal of vaporizers - Hydrogen-Air being homogeneous mixture requires no evaporation, risk of combustion in vaporizers
- nozzle position was adapted to ensure delivery of hydrogen to aerodynamically stabilized recirculation zone that anchors the flame

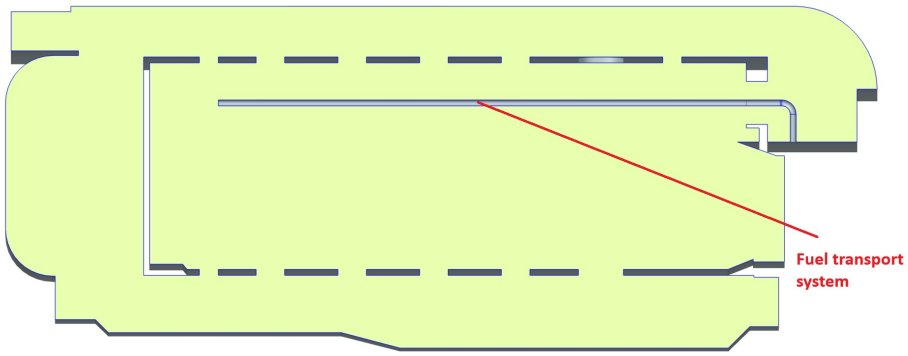

Fig 2.3 Cross-section of adapted combustion chamber - body of fluid

The designed fuel system is modeled as a constant-diameter pipe, with diameter calculated to ensure choked flow of gaseous hydrogen into the domain. Current fuel system geometry is a simplification, and will be later replaced with incorporating nozzle design and thickness of surrounding wall. Due to the periodicity of the combustion chamber geometry , the simulation takes into account only the 1/12th part, as it significantly reduces computational cost, also generating almost no error for Reynold's-Averaged NS simulation.

3 Mesh

Several options for Mesh have been considered, including coarse mesh, enabling fast and preliminary assessment of design changes. Mesh was obtained using ANSYS Mechanical software and Salome, however due to the choice of ANSYS Fluent as a software for simulation, the former was implemented because of better compatibility. In order to more accurately predict flame front and area of influence mesh adaptation over gradient of temperature was implemented. Initial mesh visualization and statistics are presented below.

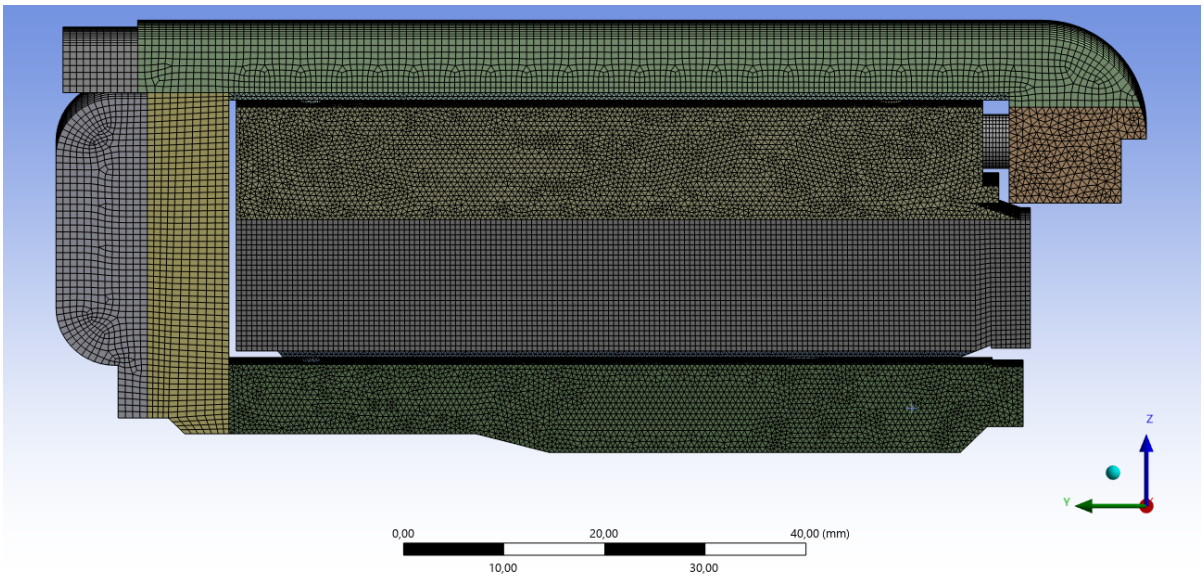

Fig. 3.1 Fluid Body Mesh Visualization

Parameter	**Value**
Nodes	646498
Elements	2645168

Tab. 3.1 Mesh Statistics

Quality of mesh was assessed according to:

1. *Aspect Ratio*

2. *Skewness*

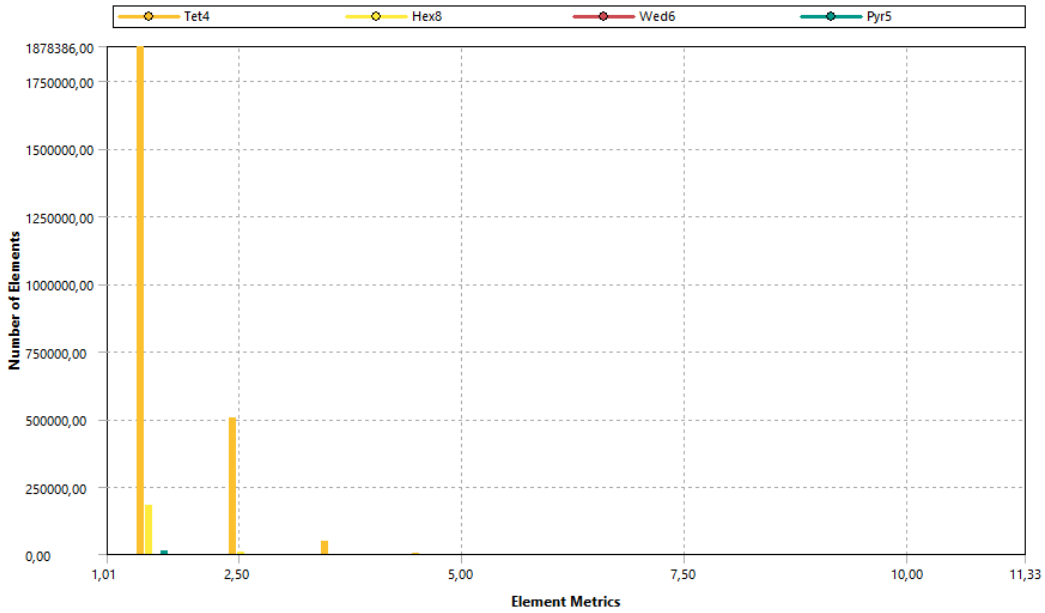

Fig 3.2 Aspect Ratio Chart

Mesh Metric	**Aspect Ratio**
Min	1.009
Max	11.328
Average	1.7905
Standard Deviation	0.47099

Tab. 3.1 Aspect Ratio Values

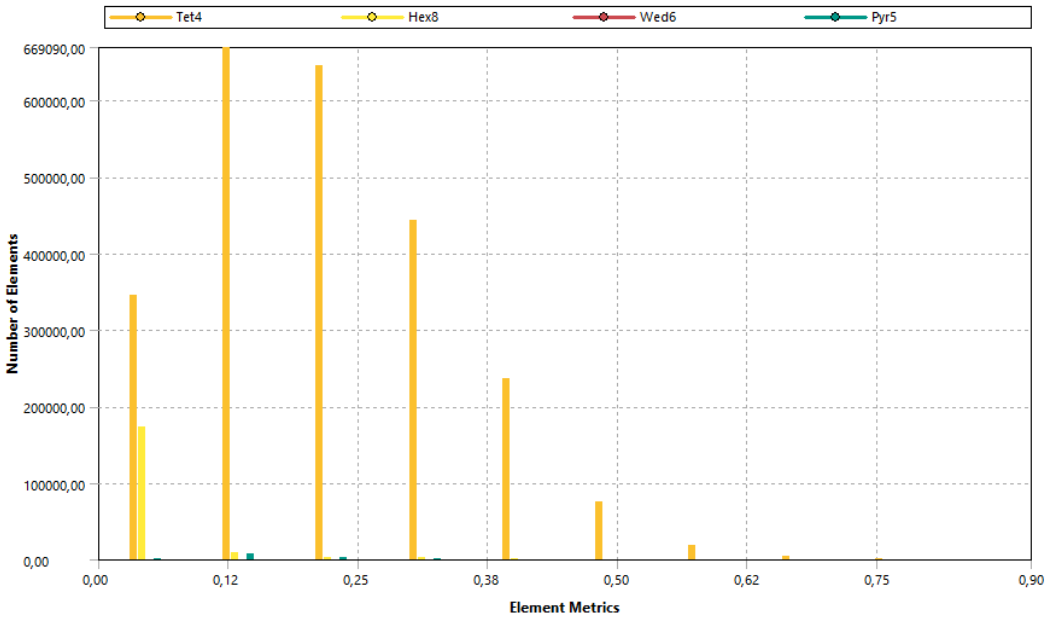

Fig. 3.3 Skewness Chart

Mesh Metric	Skewness
Min	1.063e-009
Max	0.89839
Average	0.20676
Standard Deviation	0.12681

Tab 3.2 Skewness Values

Such quality of initial mesh was accepted, even tough average value of skewness should be kept below 0.2. With highly complex geometry, including elliptically-shaped dilution holes and considering conceptual goal of simulation, such mesh enables quick adaptation to proposed geometry changes.

4 Boundary Conditions

With miniature turbine engines, extensive measurement system cannot be used, as every sensor might have significant impact on the flow and simultaneously provide unreliable data. Additionally, there isn't enough room to accommodate such systems. These are the reasons why boundary conditions might not be accurate enough to solve detailed flows, and are often assumptions, calculations using simplified models or just averaged value obtained during testing. Moreover fuel change impact on the engine as a system is yet to be assessed, therefore measurements used to predict boundary conditions are just another assumptions, assuming similar characteristics to Jet A1 powered variant with power at 100% (120000rpm).

4.1 Oxidizer Inlet

For inlet *massflow inlet* boundary condition is used, based on engine's manufacturer's data. The specification reads:

$$\dot{m}_{AirTotal} = 0.35\frac{kg}{s}$$

Considering periodicity:

$$\dot{m}_{Air} = \frac{\dot{m}_{AirTotal}}{12} = \frac{0.35}{12} = 0.029167\frac{kg}{s}$$

Studies on flow through centrifugal compressor show that assuming direction of velocity vector in diffuser area as (in this case) normal to the surface might be a source of errors, as stirring and lowering axial velocity component is crucial for proper combustion process. The components of velocity vector at the air inlet of the combustion chamber is assumed in accordance to previous simulations, done with GTM 140 engine:

$$v_{radial} = 0$$

$$v_{tangential} \approx 0.74 \cdot v_{magnitude}$$

$$v_{axial} \approx 0.67 \cdot v_{magnitude}$$

Value of $v_{magnityde}$ is computed with known mass flow rate, density and area of the air inlet

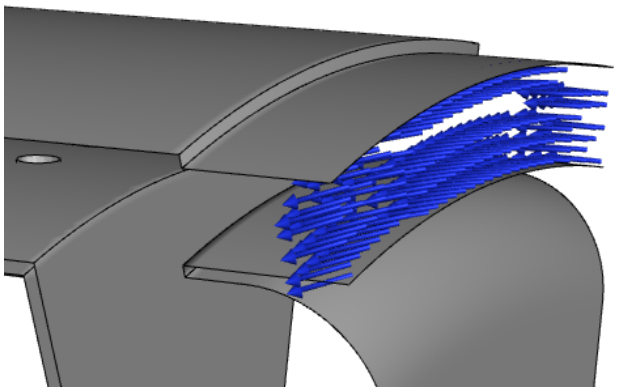

Fig 4.1.1 Inlet Velocity Vectors Visualization

Total temperature of the compressed air entering combustion chamber can be calculated in accordance to formula:

$$T_{t3} = T_{t2} \cdot \pi_c^{\frac{\kappa-1}{\kappa}}$$

- $\pi_c = 2.3$ - compression ratio
- $\kappa = 1.4$ - air specific heat ratio
- $T_{t2} = 272.1$ - total temperature for air behind inlet (chalice type, source [1])

Therefore:

$$T_{t3} = 288.17 \cdot (2.3)^{\frac{1.4-1}{1.41}} = 365.59K$$

To ensure convergence of an expected solution, additional condition for pressure was used, assuming 1 bar ambient pressure:

$$p_{inlet} = p_{ambient} \cdot \pi_c = 230000Pa$$

Turbulence was assumed using hydraulic diameter and turbulence intensity approach in $k-epsilon$ model. This approach while by no means detailed was proven to be much more accurate than default setting used in Fluent environment. For flows through ring type canals:

$$d_{hydraluic} - d_{outer} - d_{inner} = 9.26mm$$

Turbulence intensity was set to almost never used value of 15% (source [1]), however flow after going through compressor diffuser cannot be assumed developed:

$$I = \frac{\bar{u}'}{U} = 15\%$$

4.2 Fuel Inlet

Fuel inlet was also of a *massflow inlet* type. With no precedent of using hydrogen in GTM 140 engine and conceptual goal of this simulation, simplified model to calculate the value was proposed. Its base assumption is to keep an identical balance of energy for combustion chamber as in standard Jet A1 variant. Theoretical balance for combustion chamber states:

$$h_{in} + q_b = h_{out}$$

- $h_{in}[\frac{J}{kg}]$ Specific enthalpy of the components flowing into combustion chamber
- $h_{out}[\frac{J}{kg}]$ Specific enthalpy of the components flowing out of combustion chamber
- $q_b[\frac{J}{kg}]$ heat obtained from burning $1kg$ of fuel

In order to ensure that the turbine "has" available the same enthalpy to generate mechanical work and consequently provides the same compression ratio by compressor as assumed, the heat generated during combustion has to be exactly the same as in conventional configuration of the engine:

$$H_{inH_2} - H_{outH_2} = H_{inJetA1} - H_{outJetA1}$$
$$Q_{bH_2} = Q_{bJetA1}$$

knowing mass flow of a Jet A1, and lower heating value of Jet A1 and hydrogen, required mass flow of hydrogen can be calculated (assuming equal efficiency of the combustion process):

$$\dot{m}_{H_2} W_{H_2} = \dot{m}_{JetA1} W_{JetA1}$$

Using the measurement data collected during tests in KNN Melprop:

$$\dot{V}_{JetA1} = \frac{\dot{m}_{JetA1}}{\rho_{JetA1}} = 420\frac{ml}{min}$$

knowing (at T=300K):

$$\rho_{JetA1} = 791.84\frac{kg}{m^3}$$

we obtain:

$$\dot{m}_{JetA1} = 0.00558\frac{kg}{s}$$

Lower heating values for hydrogen and Jet A1 are:

- $W_{H_2} = 119.9\frac{MJ}{kg}$
- $W_{JetA1} = 42.8\frac{MJ}{kg}$

Now using previously derived formula:

$$\dot{m}_{H_2} = \frac{W_{JetA1}}{W_{H_2}} \cdot \dot{m}_{JetA1} = \frac{42.8}{119.9} \cdot 0.0058 = 0.001993\frac{kg}{s}$$

and:

$$\dot{m}_{fuel} = \frac{\dot{m}_{H2}}{12} = 0.000166\frac{kg}{s}$$

Fuel transport system diameter was calculated to ensure choked flow of hydrogen, required for uniform combustion. Previous simulations have shown that averaged pressure in combustor is approximately 210000Pa. Condition for choked flow (Mach 1) states:

$$\frac{p_{ext}}{p^*_{inj}} = \left(\frac{2}{\kappa+1}\right)^{\frac{\kappa}{\kappa-1}} = \left(\frac{2}{1.41+1}\right)^{\frac{1.41}{1.41-1}} \geq 0.5266$$

- $\kappa_{H_2} = 1.41$ - hydrogen specific heat ratio

Therefore:

$$p^*_{inj} \geq 386364Pa$$

As no contraction coefficient for nozzle was taken into account, pressure of 5 bar for hydrogen was assumed, while with higher pressure stagnation pressure value, flow would still be choked and not exceeding $Ma = 1$. Hydrogen while at $Ma = 1$, flows at the speed of over $1200\frac{m}{s}$ (assumed temperature of $310K$), for that reason it is crucial to take into consideration that it is stagnation pressure that is to exceed given value, because at this speed, dynamic pressure of hydrogen is greater than static pressure. Mass flow rate dependence on pressure, area and stagnation temperature for compressible choked flow is formulated by:

$$\dot{m} = CAp_{inj}\sqrt{\left(\frac{\kappa M}{ZRT}\right)\left(\frac{2}{\kappa+1}\right)^{\frac{\kappa+1}{\kappa-1}}}$$

- $p_{inj} = 500000Pa$ - assumed stagnation pressure for fuel transport system
- $C = 1$ - contraction coefficient presumed condition - no nozzle design is being considered
- $Z \approx 1$ - compressibility factor for hydrogen at assumed conditions
- $T = 310K$ - stagnation temperature in fuel transport system
- $M = 2,016\frac{g}{mol}$ - Hydrogen molar mass
- $R = 8314.5\frac{J}{mol \cdot K}$ - universal gas constant
- $\kappa = 1.41$

After transformation of this formula we obtain:

$$A = \frac{\dot{m}}{Cp_{inj}\sqrt{\left(\frac{\kappa M}{ZRT}\right)\left(\frac{2}{\kappa+1}\right)^{\frac{\kappa+1}{\kappa-1}}}} = 0.4326mm^2$$

now nozzle diameter can be calculated"

$$d_{nozzle} = \sqrt{\frac{4 \cdot A}{\pi}} = 0.74017mm$$

The value presented above was incorporated into the adapted geometry.

Initial turbulence was also modeled using turbulence intensity and hydraulic diameter. However in this case with high length to area ratio of hydrogen canal, fully developed turbulent flow can be assumed (typical value of turbulence intensity):

- $I = \frac{\bar{u'}}{U} = 5\%$
- $d_h = d_{nozzle} = 0.74017mm$

4.3 Outlet

Outlet was modeled as *pressure outlet*. The averaged value of outlet pressure was taken, based on measurements done by KNN Melprop for GTM 140 engine:

$$p_{outlet} = 190000Pa$$

to accelerate convergence of the solution, other variables were assumed (backflow conditions), however these values as not treated by solver as fixed boundary conditions:

- $T_{backflow} = 862K$
- $I_{backflow} = 15\%$
- $d_{hbacklow} = d_{outer-back} - d_{inner-back} \approx 26mm$

5 Combustion model

Taking into account complexity of combustor geometry, coarse mesh, and conceptual characteristic of simulation *non-premixed combustion* model was used instead of much more direct, less stable and computationally demanding *species transport*, which was proven unstable while solving this case in *reactingFoam* solver using Openfoam. However instead of default equilibrium state calculations, one dimensional freely-propagating laminar unsteady flamelet model was generated using embedded *Chemkin* solver and Probability Density Function. The basis for this calculation was reduced mechanism of hydrogen-air combustion developed by San Diego University. The mechanism includes 9 species:

1. H_2 (Hydrogen)
2. O_2 (Oxygen)
3. H (Atomic Hydrogen)
4. O (Atomic Oxygen)
5. OH (Hydroxyl Radical)
6. H_2O (Water)
7. HO_2 (Hydroperoxyl Radical)
8. H_2O_2 (Hydrogen Peroxide)
9. N_2 (Nitrogen - Inert)

and 21 reactions:

$$\mathrm{H + O_2 \rightleftharpoons OH + O} \tag{1}$$
$$\mathrm{H_2 + O \rightleftharpoons OH + H} \tag{2}$$
$$\mathrm{H_2 + OH \rightleftharpoons H_2O + H} \tag{3}$$
$$\mathrm{H_2O + O \rightleftharpoons 2\,OH} \tag{4}$$
$$\mathrm{2\,H + M \rightleftharpoons H_2 + M} \tag{5}$$
$$\mathrm{H + OH + M \rightleftharpoons H_2O + M} \tag{6}$$
$$\mathrm{2\,O + M \rightleftharpoons O_2 + M} \tag{7}$$
$$\mathrm{H + O + M \rightleftharpoons OH + M} \tag{8}$$
$$\mathrm{O + OH + M \rightleftharpoons HO_2 + M} \tag{9}$$
$$\mathrm{H + O_2\,(^+M) \rightleftharpoons HO_2\,(^+M)} \tag{10}$$
$$\mathrm{HO_2 + H \rightleftharpoons 2\,OH} \tag{11}$$
$$\mathrm{HO_2 + H \rightleftharpoons H_2 + O_2} \tag{12}$$
$$\mathrm{HO_2 + H \rightleftharpoons H_2O + O} \tag{13}$$
$$\mathrm{HO_2 + O \rightleftharpoons OH + O_2} \tag{14}$$
$$\mathrm{HO_2 + OH \rightleftharpoons H_2O + O_2} \tag{15}$$
$$\mathrm{2\,OH\,(^+M) \rightleftharpoons H_2O_2\,(^+M)} \tag{16}$$
$$\mathrm{2\,HO_2 \rightleftharpoons H_2O_2 + O_2} \tag{17}$$
$$\mathrm{H_2O_2 + H \rightleftharpoons HO_2 + H_2} \tag{18}$$
$$\mathrm{H_2O_2 + H \rightleftharpoons H_2O + OH} \tag{19}$$
$$\mathrm{H_2O_2 + OH \rightleftharpoons H_2O + HO_2} \tag{20}$$
$$\mathrm{H_2O_2 + O \rightleftharpoons HO_2 + OH} \tag{21}$$

Reactions containing $(^+\mathrm{M})$ are falloff reactions and those containing $+\mathrm{M}$ are three body reactions with specified efficiencies. For very reactions listed, 3 modified Arrhenius's equation coefficients has been assigned A; b; E:

$$k = AT^b exp(-\frac{E}{RT})$$

For every species used thermodynamical properties data was provided in the form of NASA polynomials coefficients. NASA polynomials formulates dependency of heat capacity, enhropy and enthalpy respectively on temperature:

$$\frac{C_p}{R} = a_1 + a_2T + a_3T^2 + a_4T^3 + a_5T^4$$

$$\frac{H}{RT} = a_1 + \frac{a_2T}{2} + \frac{a_3T^2}{3} + \frac{a_4T^3}{4} + \frac{a_5T^4}{5} + \frac{a_6}{T}$$

$$\frac{S}{R} = a_1ln(T) + a_2T + \frac{a_3T^2}{2} + \frac{a_4T^3}{3} + \frac{a_5T^4}{4} + a_7$$

Initial Mass fractions assigned are respectively:

- $C_{O_2} = 21.008\%$
- $C_{N_2} = 78.992\%$

for oxidizer inlet, and

- $C_{H_2} = 100\%$

for fuel inlet.

6 Solver settings

Solver, solution and relaxation factors setting are listed in tables below:

Parameter	**Option**
Solver	Pressure-Based
Time	Steady
Velocity Formulation	Absolute
Viscous Model	k-epsilon Realizable
Near Wall Treatment	Standard Wall Function
Species	Non-Premixed Combustion
Radiation	Discrete Ordinates

Tab. 6.1 Solver settings and used models

Parameter	**Option**
Pressure-Velocity Coupling	Coupled
Gradient	Least Square Cell Based
Pressure	Second Order
Density	First Order Upwind
Momentum	First Order Upwind
Turbulent Kinetic Energy	First Order Upwind
Turbulent Dissipation Rate	First Order Upwind
Energy	Second Order Upwind
Discrete Ordinates	First Order Upwind
Mean Mixture Fraction	Second Order Upwind
Inertial-Convective Variance	First Order Upwind
Viscous-Convective Variance	First Order Upwind
Viscous-Diffusive	First Order Upwind

Tab. 6.2 Numerical schemes

Parameter	Value
Pressure	0.5
Density	1
Body Forces	1
Momentum	0.5
Turbulent Kinetic Energy	0.8
Turbulent Dissipation Rate	0.8
Turbulent Viscosity	1
Energy	1
Temperature	1
Discrete Ordinates	1
Mean Mixture Fraction	1
Inertial-Convective Variance	0.9
Viscous-Convective Variance	0.9
Viscous-Diffusive	0.9

Tab. 6.3 Relaxation factors

Coupled pressure-momentum coupling method was applied, as treating pressure and momentum as single systems, was found easier to converge, despite higher computational cost then *SIMPLE* and its variation - *PISO* method. Additionally, most of the variables initially used First Order Upwind, and were switched later during the solving to Second Order Upwind. Initial iteration number was set to 300. On top of residuals tracked by default on the basis of used equations, tracking mass flow, flowing out of pressure outlet was checked.

Solution took approximately 5 hours using 18 cores - dual processor KNN Melprop's workstation. Convergence criteria were not satisfied, however residuals values were assessed to be low enough considering once again conceptual nature of calculations , and continuing calculations would lower them significantly,

7 Mesh Adaptation

Prior combustion simulation has shown an importance of mesh refinement in order to better predict flame front and combustion zone. For considered flow with combustion, it is value of gradient of temperature that was applied as a criteria to refine mesh. Initial unadapted solution provided temperature gradients ranging form 0 to 1300. The value of 200 was selected as a value triggering refinement. Maximal refinement factor was set to default value of 2. Each of 4 mesh refinement was done after 100-iteration, convergence-checking calculation. The one-adaptation form of mesh is presented below:

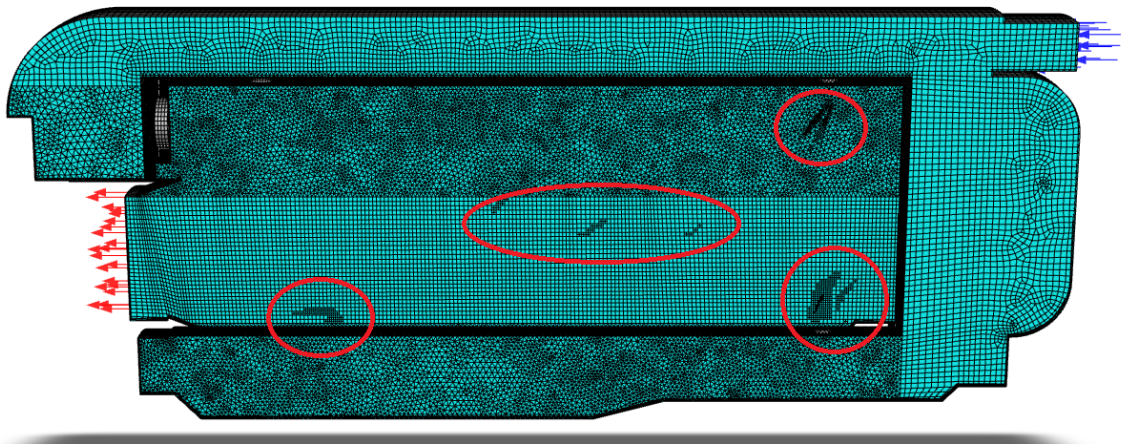

Fig 7.1 Refined mesh regions

8 Results

All of the results are presented as graphs and contour plots. The letter are plots of variable fields on symmetry plane to visualize the flow around fuel transport system.

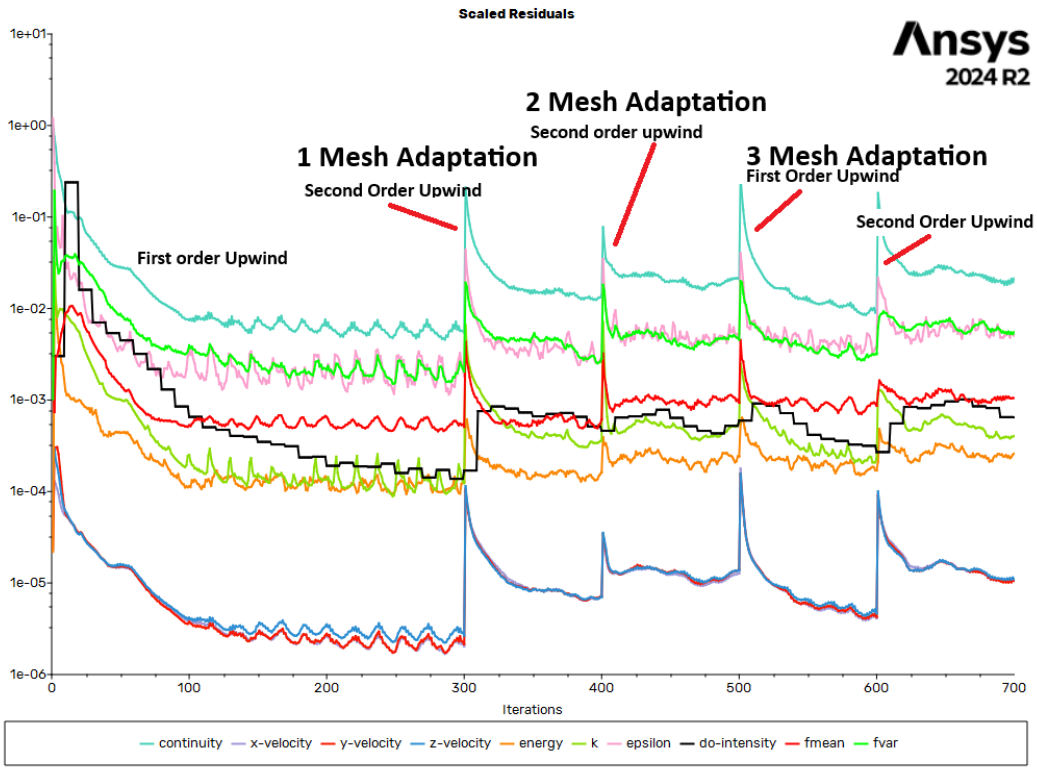

Fig. 8.1 Residuals values

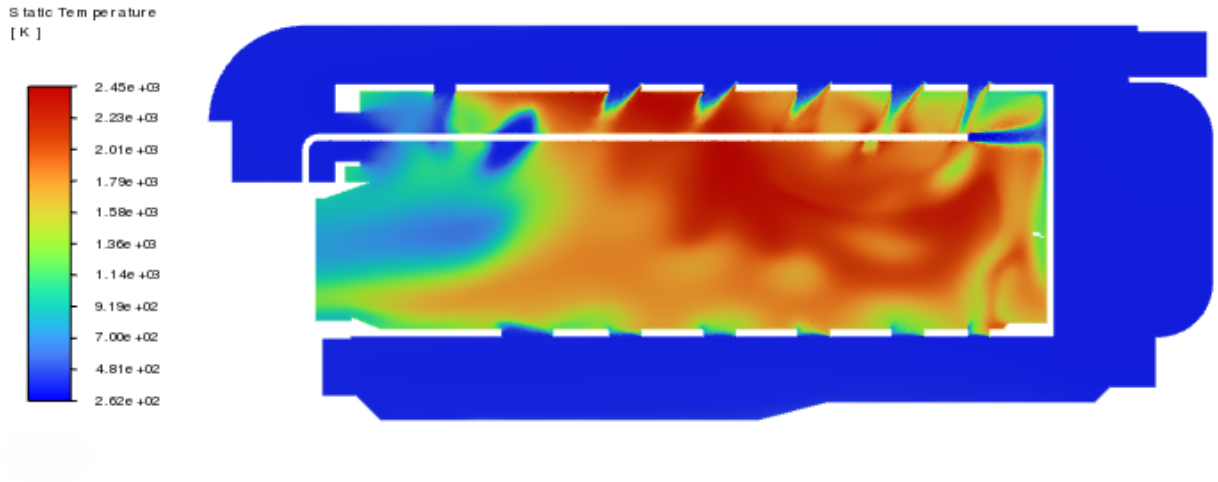

Fig. 8.2 Static Temperature contour

Fig. 8.3 Velocity Magnitude contour

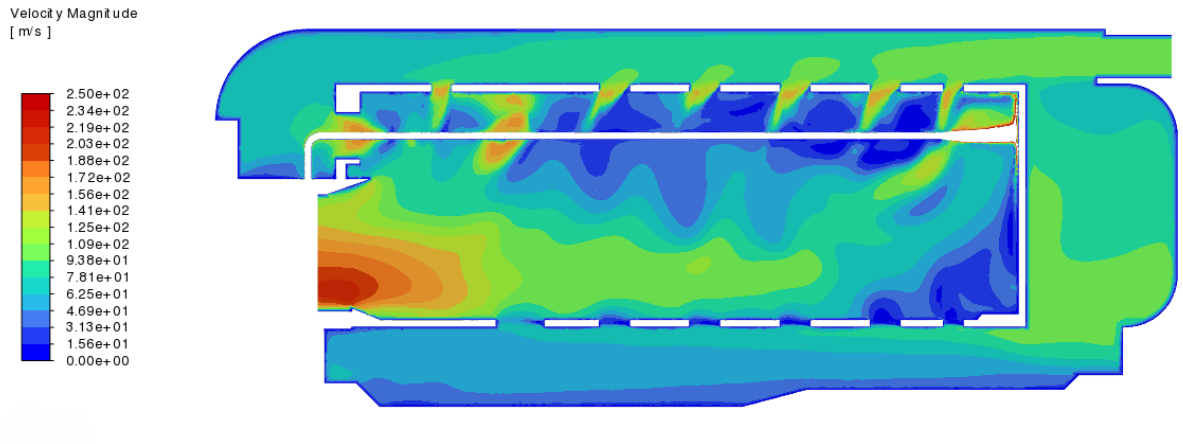

Fig. 8.4 Velocity Magnitude contour - limited to 250 m/s

Fig. 8.5 Static Pressure contour

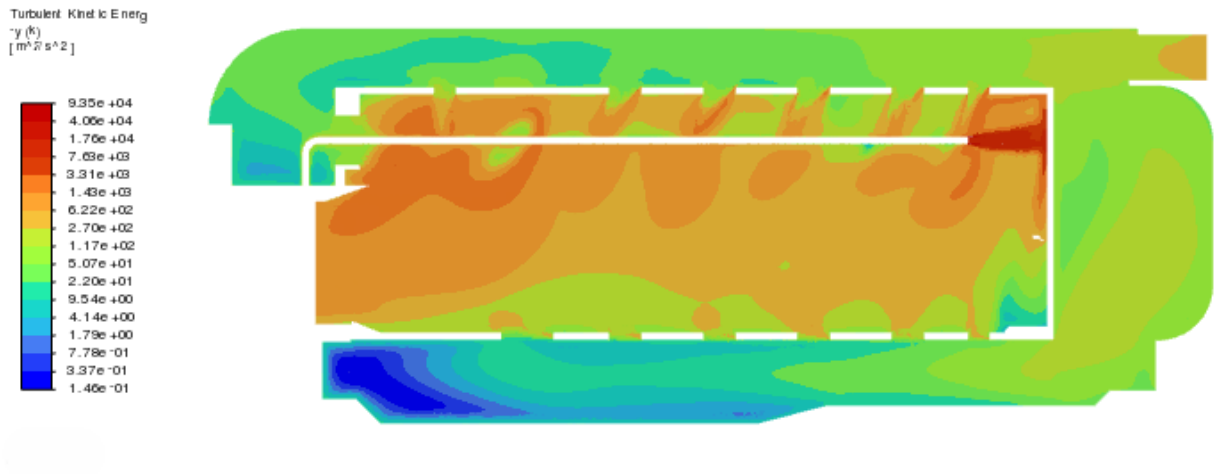

Fig. 8.6 Turbulence Kinetic Energy contour - logarithmic scale

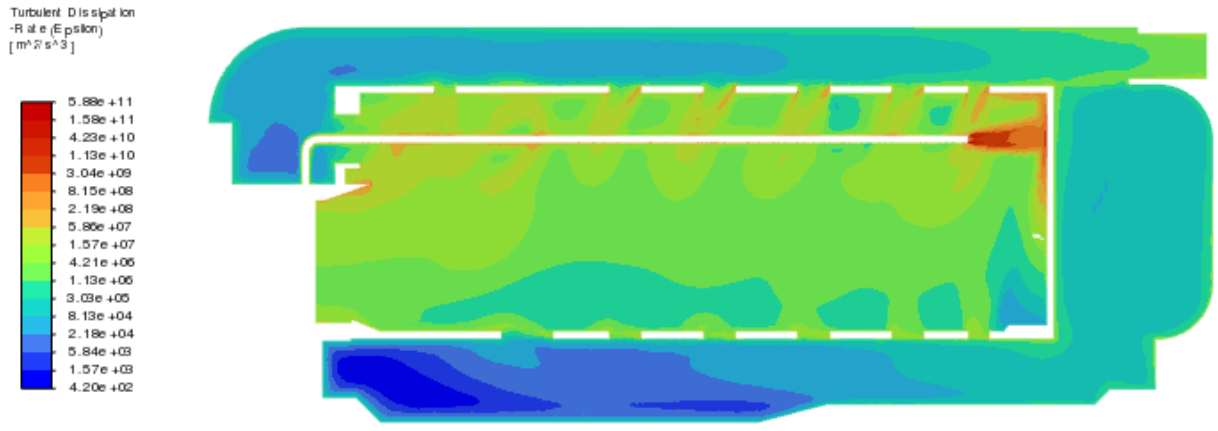

Fig. 8.7 Turbulence Dissipation Rate contour - logarithmic scale

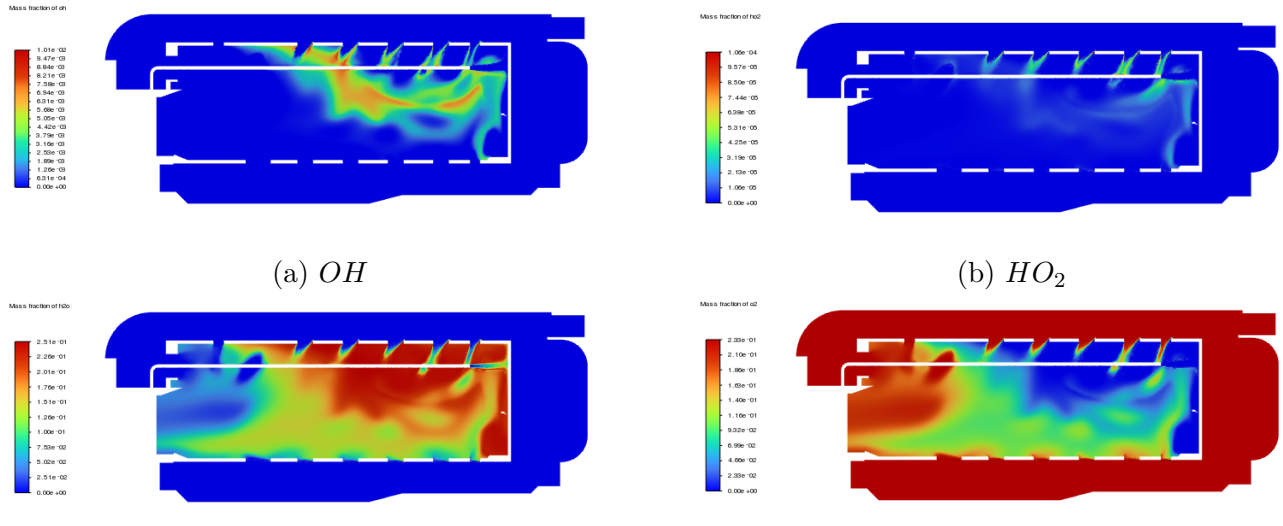

(a) OH (b) HO_2

(c) H_2O (d) O_2

Fig 8.8 Mass Fractions of Species - contour, for visualization purposes

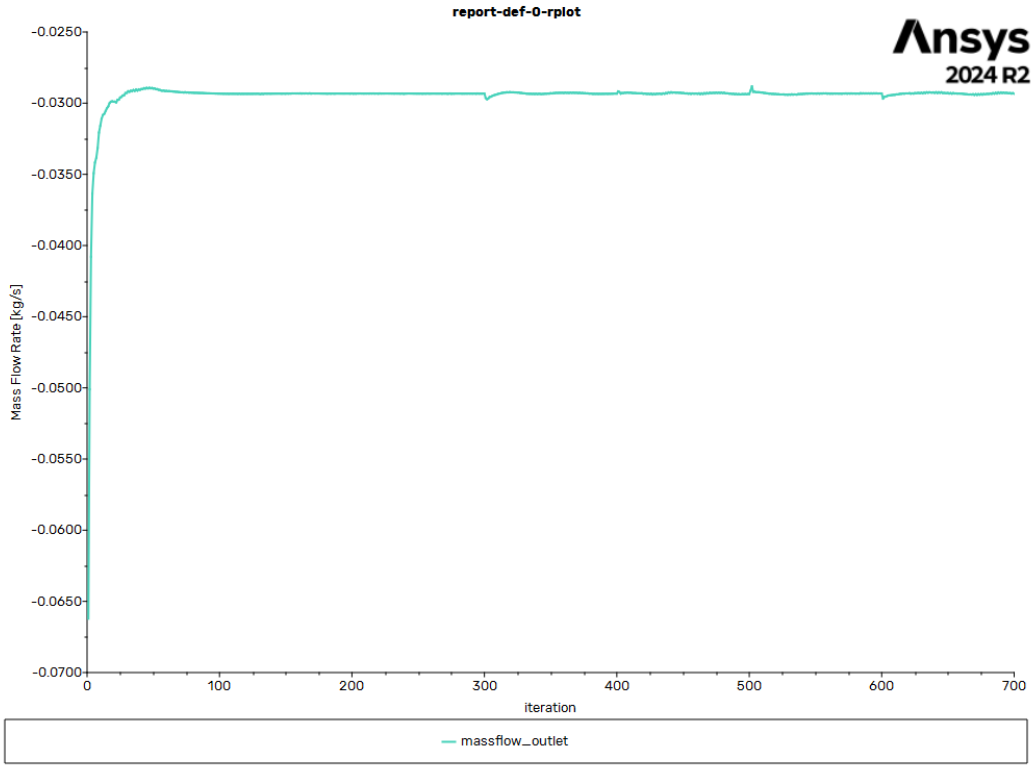

Fig. 8.9 Mass Flow Rate at Outlet

9 Conclusions

1. In comparison to Jet A1 higher temperature values were expected. The maximum value is 2450K which can be lowered by including NO_x production mechanisms such as Zeldovich

mechanism and prompt mechanism, another source of lowering temperature can be inclusion of heat transfer between combustor and the agent. Current values are unacceptable, especially considering melting temperature of materials used in combustor such as incandescent steel and even Inconel 718 - proposed for fuel transport system. Also fuel composition can be changed, as Hydrogen - Methane mixtures were proven to have lower maximal temperatures, while both components have similar mixing length. However such engine would no longer be free of CO_2 emissions.

2. Static temperature contour and velocity vector field show deleting vaporizer made flow significantly cooled before exiting combustion chamber. It can be beneficial considering materials durability (especially turbine), however it causes engine as a system to be less efficient, as efficiency of the thermodynamic cycle (Joul-Bryton) is proportional to the square root of averaged total temperature before entering turbine. Measured outlet average temperature was $T_{t4} = 960K$, which is high enough. In order to make lower fuel consumption design changes should be implemented and mass flow of hydrogen accordingly reduced.

3. With hydrogen being faster to mix than Jet A1 (also required evaporation), it is not necessary to inject fuel in opposed direction, however flame detachment possibilities should be considered in case of injection being the same direction as the main flow.

4. As hydroxyl radical is universally used in measurements technics as way of detecting zone of combustion, design changes for GTM 140 combustion chamber should be made accordingly.

5. More design changes shall be considered to address the issue of combustion chamber adaptation. However, to ensure improved efficiency over Jet A1 variant, complete redesign of geometry and new means of "shaping" the flow (stabilization) are required.

6. Results should be assessed in therms of numerical errors.

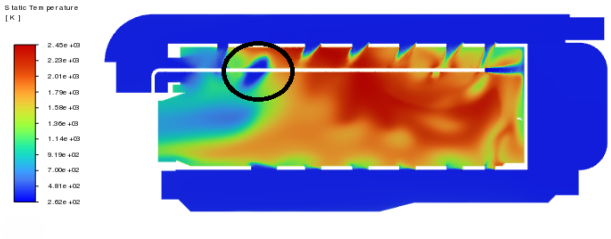

Fig. 9.1 Numerical error - non-physical value of temperature considering surrounding field

10 References

1. Gieras M.: *Miniaturowe silniki turbinowe*, Oficyna Wydawnicza Politechniki Warszawskiej, Warszawa 2016

2. Suchocki T. K., Lampart P.: *Ocena Modyfikacji Układu Parownic oraz Otworów Chłodzących Turbiny Gazowej GTM-140*, XIX Międzynarodowa Szkoła Komputerowego Wspomagania Projektowania, Wytwarzania i Eksploatacji - MECHANIK 7/2015

3. Gieras M., Chmielewski M. :*Badania Wpływu Zmian Geometrii Komory Spalania Na Efektywność Procesów Spalania i Emisję Substancji Szkodliwych w Miniaturowej Turbinie Gazowej*,

4. Kee R.J., F.M. Rupley, Miler J.A.:*The Chemkin Thermodynamic Data Base*, 1990